Original Article

Mice lacking α1,3-fucosyltransferase 9 exhibit modulation of *in vivo* immune responses against pathogens

Hiromi Kashiwazaki,[1] Masatoshi Kakizaki,[1] Yuzuru Ikehara,[2] Akira Togayachi,[2] Hisashi Narimatsu[2] and Rihito Watanabe[1]

[1]*Department of Bioinformatics, Faculty of Engineering, Soka University, Hachioji, Tokyo and* [2]*Research Center for Medical Glycoscience, National Institute of Advanced Industrial Science and Technology (AIST), Tsukuba, Ibaraki, Japan*

Carbohydrate structures, including Lewis X (Le^x), which is not synthesized in mutant mice that lack α1,3-fucosyltransferase 9 (Fut9$^{-/-}$), are involved in cell–cell recognition and inflammation. However, immunological alteration in Fut9$^{-/-}$ mice has not been studied. Thus, the inflammatory response of Fut9$^{-/-}$ mice was examined using the highly neurovirulent mouse hepatitis virus (MHV) JHMV srr7 strain. Pathological study revealed that inflammation induced in the brains of Fut9$^{-/-}$ mice after infection was more extensive compared with that of wild-type mice, although viral titers obtained from the brains of mutant mice were lower than those of wild-type mice. Furthermore, the reduction in cell numbers in the spleens of wild-type mice after infection was not observed in the infected Fut9$^{-/-}$ mice. Although there were no clear differences in the levels of cytokines examined in the brains between Fut9$^{-/-}$ and wild-type mice except for interferon-β (IFN-β) expression, some of those in the spleens, including interferon-γ (IFN-γ), interleukin-6 (IL-6), and monocyte chemoattractant protein-1 (MCP-1), showed higher levels in Fut9$^{-/-}$ than in wild-type mice. Furthermore, Fut9$^{-/-}$ mice were refractory to the *in vivo* inoculation of endotoxin (LPS) compared with wild-type mice. These results indicate that Le^x structures are involved in host responses against viral or bacterial challenges.

Key words: cytokine, Fut9, Lewis X, MHV, neuropathogenic virus

Murine coronavirus mouse hepatitis virus (MHV) is an enveloped virus.[1] Infection in most tissues is thought to be mediated by a major MHV receptor (MHVR), carcinoembryonic antigen-related cell adhesion molecule 1 (CEACAM 1).[2,3] From the neurovirulent MHV strain JHMV, highly neuropathogenic cl-2[4] and less virulent srr7 viruses (srr7) have been isolated,[5] which exhibit super acute spread of virus (SAS), a term applied when rapid viral spread from one organ or part of the initially infected site to another non-adjacent organ or part is detected within 12 h after infection.[6,7] Although srr7 shows slightly reduced virulence compared to its maternal virus cl-2, it still exhibits high-level virulence, causing the death of mice within 10 days after infection. Initial viral antigens can already be detected at 12 h post-inoculation (hpi) either with cl-2 or srr7 in infiltrating cells that appear in the subarachnoidal space and spleen at the same time. All kinds of splenic cells examined were infected.[7] In spite of wide-spread lesions accompanied by viral antigen distribution in the parenchyma of the central nervous system, the inflammatory response is minimal except for in the meningeal area.[6,8] Besides the neuropathogenicity, srr7 and cl-2 cause marked cell depletion in the spleen after infection.[7] At 24 hpi, the population of leukocytes in the spleen becomes less than 50% of the splenic cell number of uninfected mice, but the reason remains unclear because the infected cell number in the spleen is too small to account for the reduction.

Recently, interest in the pathogenicity of coronaviruses has increased markedly because of newly emergent coronaviruses, which cause severe acute respiratory syndrome (SARS)[9] and Middle East respiratory syndrome (MERS)[10] in humans. Murine coronaviruses, particularly MHV, have been used to develop a number of informative animal models to elucidate their highly mutative nature causing different pathogenesis[11,12] and the mechanisms of acute spread of the viruses.[1,6,7] However, studies on the acute phase of infection with MHV have been lacking.[1]

In this study, we investigated whether characteristics of the pathology can be changed by modifying the pattern of the

carbohydrate structure of the host animals, which contributes to viral infectivity,[13] including MHV infection[14,15] and immune system function.[13] The studies were carried out with particular relevance to innate immunity, using Fut9$^{-/-}$ mice,[16] which lack α1,3-fucosyltransferase 9 and are unable to synthesize the Lewis x (Le^x) structure, because srr7 induces neuropathological lesions during the early phase of infection before adaptive immune responses occur, and the Le^x structure is believed to be involved in innate immunity through cell–cell- and pathogen-recognition.[17–19] The treatment of patients infected with highly virulent viruses during the early phase of infection includes the control of excessive innate immune responses with or without inflammatory pictures, the latter of which is observed typically in encephalopathy induced by influenza viral infection.[20] Furthermore, Le^x and Fut9 are highly expressed in the central nervous system (CNS).[21,22] In addition, Fut9$^{-/-}$ mice develop normally without gross phenotypic abnormalities in the brain and other organs,[16,22] which might affect pathological changes induced by neuropathogenic viral infection.

Although interactions through fucosylated glycans play important roles in innate immunity, of which inhibition has been investigated as an attractive target of anti-inflammatory therapy,[19,23,24] there have been no reports on host immune responses against infection after the inhibition of *in vivo* fucosylation. Our study demonstrated that immunomodulation during the phase of innate immunity occurred in Fut9$^{-/-}$ mice.

MATERIALS AND METHODS

Treatment of mice

The Fut9$^{-/-}$ mice with a BALB/c background[16] and BALB/c mice purchased from Charles River (Tokyo, Japan) were housed in a specific pathogen-free animal facility, and were kept according to the guidelines set by the committee of our university and National Institute of Advanced Industrial Science and Technology (AIST). For infection, mice were transferred to the P3-level laboratory. Each mouse was injected with 1×10^2 of the srr7 virus[5] in 50 μL of culture medium into the right frontal lobe under deep anesthesia, or left untreated. Some mice were injected into the hind footpad with 10 μg of lipopolysaccharide (LPS, *Escherichia coli* strain 0111:B4; Sigma, Tokyo, Japan) in 50 μL of PBS.

Pathology

Immunostaining was carried out using the antibodies and reagents listed in Table 1. Sections labeled with immunofluorescence were mounted with gold antifade reagent (Invitrogen, Carlsbad, CA, USA) and examined using a fluorescence microscope (Keyence, Osaka, Japan) or confocal laser scanning microscope (Leica Microsystems, Heidelberg, Germany). Tissues for pathological examination were prepared as previously reported.[8] The intensities of inflammation and hyperplastic or atrophic states of the spleen were scored according to the criteria outlined in Methods S1.

The size of the lymph nodes was determined by measuring the largest cross-sectional area of a hematoxylin and eosin (HE)-stained lymph node using the BZ analyzer (Keyence).

Infection of peritoneal exuding cells

Four days after the injection of 4% thioglycolate into the peritoneal cavity, the exuding cells collected after washing the peritoneal cavity were seeded at 2×10^4 cells per well in eight-well plastic chamber slides (Nalge Nunc International, Rochester, NY, USA), and were cultured overnight under the same conditions as splenic cells described below. Adherent cells were inoculated with 10 PFU (plaque-forming units) of

Table 1 Antibodies and reagent used in this study

Target	Species	Clone or designation	Conjugate	Reference/supplier
Primary antibodies for immunofluorescence staining of murine tissue sections				
JHMV	Mouse	Monoclonal	Purified	3
CD11b	Rat IgG2b, κ	M1/70	Biotin	BD Pharmingen, San. Diego, CA, USA, 557395
CD20	Goat	M-20	Purified	Santa Cruz Biotechnology, Santa Cruz, CA, USA, sc-7735
IFN-β	Rabbit	Polyclonal	Purified	PBL Interferon Source, Piscataway, NJ, USA, 32400-1
Secondary antibodies for immunofluorescence staining of murine tissue sections				
Anti-mouse IgG	Goat	Polyclonal	Alexa488	Molecular Probe, Carlsbad, CA, USA
Anti-mouse IgG	Donkey	Polyclonal	Biotin	Rockland, Gilbertsville, PA, USA, 610-706-124
Anti-goat IgG	Donkey	Polyclonal	Alexa488	Invitrogen, Carlsbad, CA, USA, A11055
Anti-rabbit IgG	Goat	Polyclonal	Alexa568	Invitrogen, A11011
Streptavidin			Alexa568	Invitrogen, S11226
Streptavidin			Horseradish peroxidase	Zymed, South San Francisco, CA, USA, 43-4323
Reagent to stain nuclei				
Hoechst 33342				Invitrogen, H21492

srr7 virus per well and incubated for the specified time period. Viral antigen-positive cells were visualized by immunofluorescence, as described above.

Cytokine assay

Protein from the pons and spleen was purified according to the manufacturer's instructions (Affimetrix, Santa Clara, CA, USA), with minor modifications using radio-immunoprecipitation assay buffer (Wako, Osaka, Japan) in addition to cell lysis buffer (Affimetrix). Experimental details are described in Methods S1.

Statistical analysis

Overall survival (Fig. 1a) was analyzed and compared by the Kaplan–Meier method. Differences in survival were tested for significance by the log-rank test. Otherwise, Student's *t* test was used. *P*-values of less than 0.05 were considered to indicate significance.

RESULTS

Viral growth and virulence

Although mutant mice showed a slightly shorter survival period after infection, no fundamental differences in virulence among the different strains of mice after infection were observed (Fig. 1a), showing that infected mice died within 10 days post-inoculation (dpi). Viral titers prepared from organs of infected mice at desired time-points are shown in Fig. 1b. Viral growth in the mutant mice was more than one order lower compared with that in wild-type mice (Fig. 1b).

Pathological findings

Prominent inflammation extending to the brain parenchyma was observed in infected mutant mice (Fig. 2a). In contrast, cell infiltration was restricted to the perivascular area to a less extensive degree in infected wild-type mice (Fig. 2b) except for the meningeal region, which was already observed at 48 hpi both in mutant and wild-type mice (Fig. 3a,b), as we reported previously.[6,8,25] Cell infiltration beyond the Virchow-Robin space (arrowheads in Fig. 2a) was observed more frequently in the brain parenchyma of mutant mice than that of wild-type mice (Fig. 4a), already at 48 hpi. The distribution of viral antigens in the brains of mutant mice appeared in a similar manner to that of wild-type mice, as previously reported.[6,8] During the early phase of infection, at 48 hpi, viral antigens were detected in the meninges (Fig. 3a,b), which appeared at a similar frequency in mutant and wild-type mice (Fig. 3c), and in the restricted area in the periventricular area (Fig. 2c,e). During the later phase of infection, they were distributed in the wide areas of the brain of mutant mice in the same manner as those found in wild-type mice (Fig. 2d,f).

The splenic lesions observed in infected wild-type mice, characterized by the depletion of leukocytes (Fig. 2i,4b), numbers of which reduced to less than 50% of those of uninfected wild-type mice at 48 hpi,[7] with many apoptotic figures (white arrows in Fig. 2j), which already appeared at 24 hpi (data not shown), accompanied by hemosiderin deposits (black arrows in Fig. 2j), were not apparent in infected mutant mice (Fig. 2h). The spleens of infected mutant mice at 24 and 48 hpi showed rather hyperplastic states (Figs 2g,4b), with clusters of leukocytes (arrows in Fig. 2h), mainly composed of CD11b-positive cells (Fig. 3d,e), in the interfollicular areas. The appearance of viral antigens during the early phase of infection (48 hpi) in the spleens was observed at a similar frequency (Fig. 3c). Similar infectivities of the two strains were also detected in an *in vitro* assay (Fig. 1c), using peritoneal exuding cells after challenge with thioglycolate, which were composed mainly of MHV-susceptible CD11b-positive cells (>99%, data not shown).

Cytokine assay and LPS challenge

There were almost no differences between mutant and wild-type mice in the shift of cytokine levels after infection examined in the pons and spleen, except for IFN-β in the pons, and IFN-γ, IL-6 and MCP-1 in the spleen (Fig. 5). JHM viruses are known to proliferate, suppressing the production of IFN-β in the *in vitro*-infected cells.[26–28] Because IFN-β levels in the pons were increased after infection both in mutant and wild-type mice, we examined IFN-β expression by immunofluorescence, and IFN-β was found to be widely distributed in the brain parenchyma, where viral antigens were not detected at 48 hpi, although many infected cells had infiltrated the meninges, as shown in the upper left corner of Fig. 3f. The result indicated that the IFN-β after infection is considered to be produced by an indirect bystander effect on the cells in the brain parenchyma.

Inoculation of LPS *in vivo* also showed different inflammatory responses between mutant and wild-type mice. A marked reduction in the size of the popliteal lymph nodes (pLN) with inoculation of LPS and infection of wild-type mice compared to that only with LPS was observed (Fig 4c), and such a reduction did not occur in mutant mice. However, mutant mice were shown to be refractory to the LPS challenge (Fig. 4c). The possibility that this refractoriness in mutant mice is a result of the poor recognition of LPS is

(a)

(b)

(c)
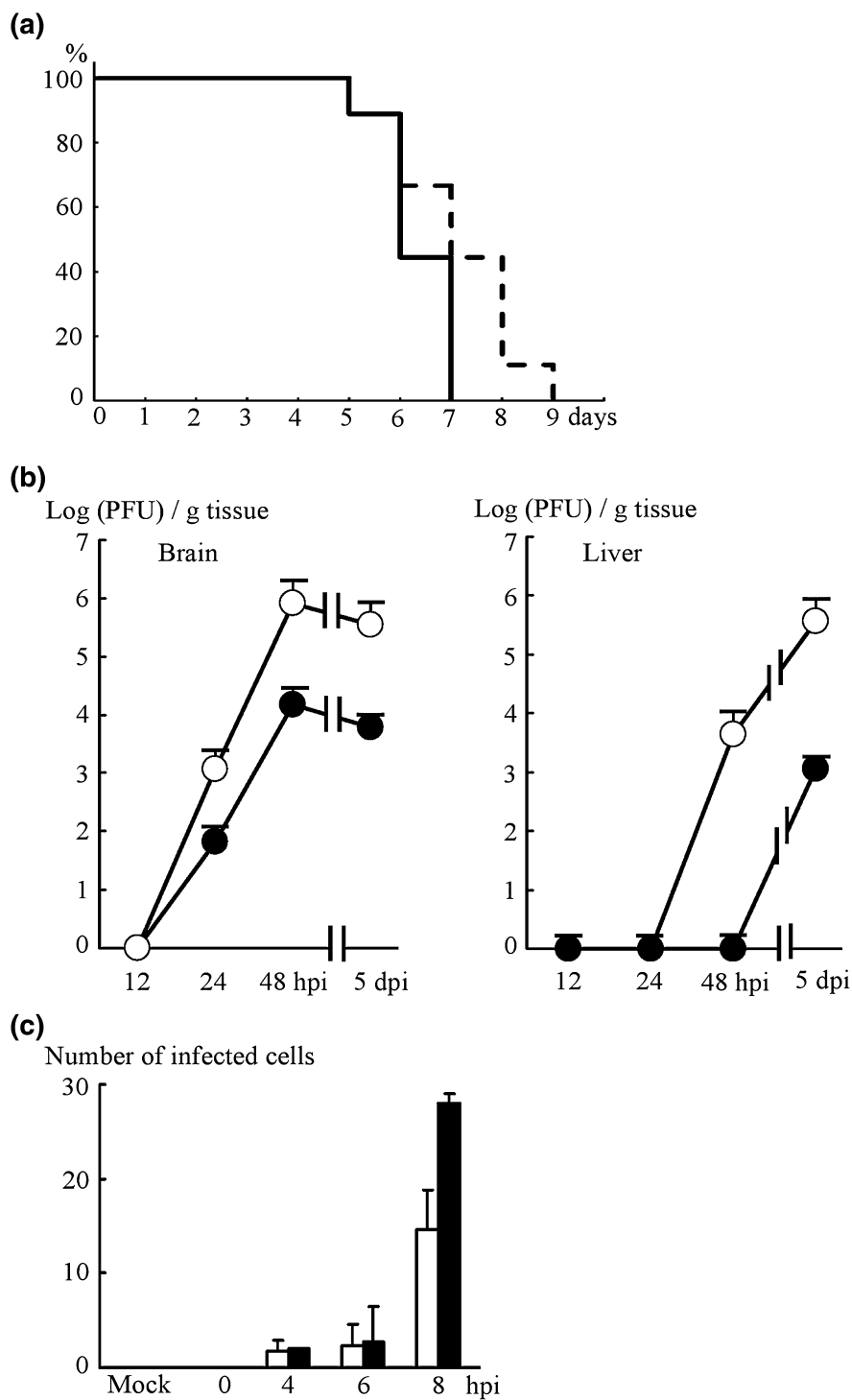
Figure 1 Kaplan-Meier survival curves (**a**) and viral titration in the brain and liver (**b**) after infection in mutant (fBA, closed circles) and wild-type (wBA, open circles) mice. (**a**) Numbers in parenthesis indicate the number of mice examined. The *P*-value between the two strains analyzed by the log-rank test was 0.07. (**b**) Viral titers were measured as plaque-forming units (PFU) per one gram of the brain or liver. The standard deviation is shown by the vertical line. The *P*-value (p) by Student's t-test is shown as *, which indicates $P < 0.05$. (**c**) Percentages of infected cells at the times indicated after infection with srr7. Each infection was conducted in triplicate and viral antigen-positive cells were counted for each well. (**a**) - - -: wBA; ——: fBA. (**b**) ○, wBA; ●, fBA. (**c**) □, wBA; ■, fBA.

unlikely, because leukocytes derived from mutant mice produced higher levels of some cytokines after stimulation with LPS *in vitro* than those from wild-type mice (Fig. S1). Elucidation of the mechanism needs further studies, including migration rates of leukocytes into pLN, which might be low in mutant mice after the challenge, because the infected cells in pLN were much fewer (Fig. 3c), counted as less than 25–50% compared to those of wild-type mice (Fig. 3c). Many viral antigen-positive cells were mainly detected in the interfollicular area of pLN obtained from infected wild-type mice after inoculation with LPS (Fig. 3i), whereas few viral antigen-positive cells were detected within the LN parenchyma of infected wild-type mice untreated with LPS or mutant mice (Fig. 3g,h).
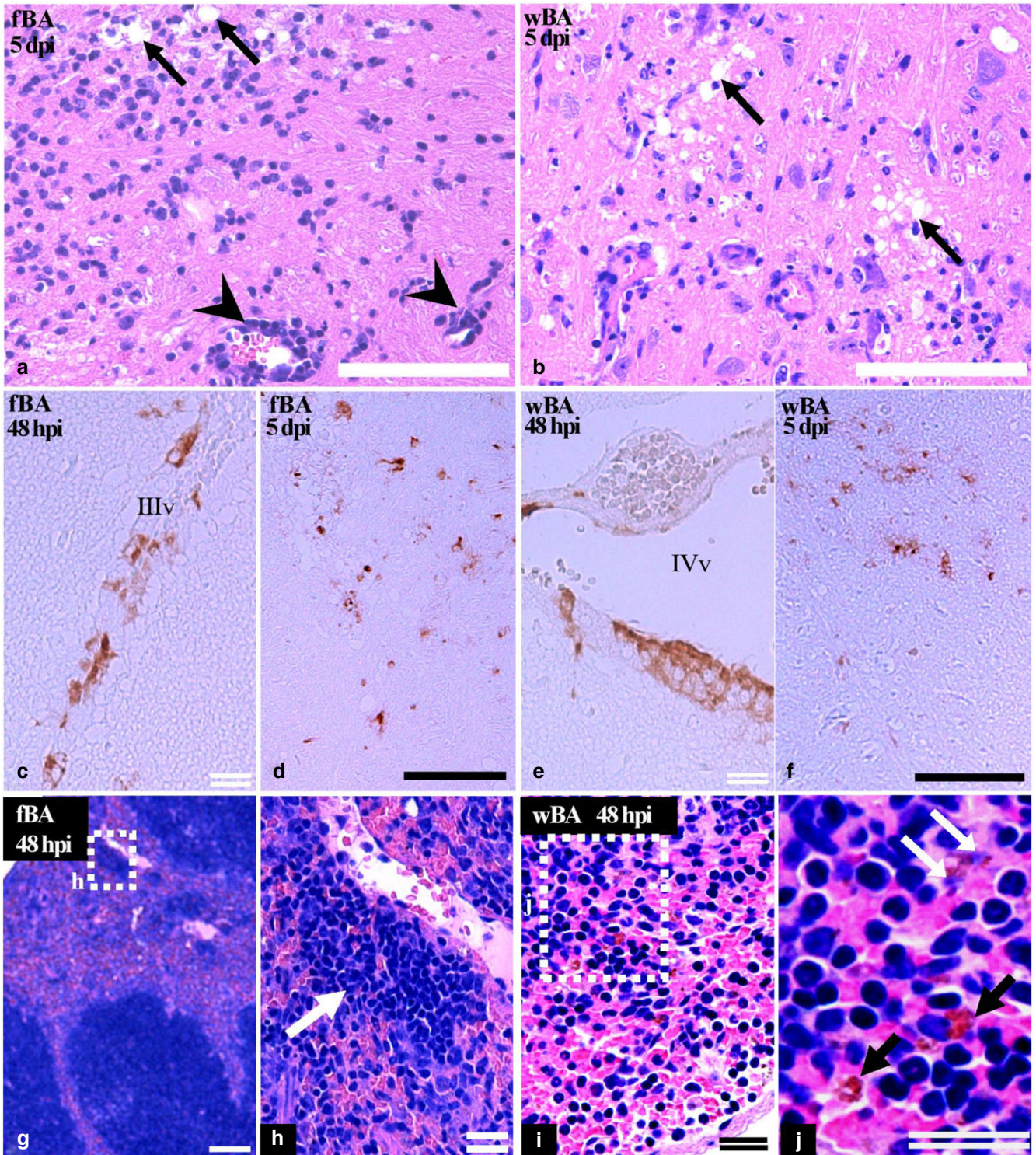
Figure 2 Paraffin-embedded sections (**a–j**) obtained from the pons (**a,b**), thalamus (**d,f**) around the third (IIIv) and fourth ventricle (IVv), respectively (**c,e**), and spleen (**g–j**) were stained with HE (**a, b, and g–j**), for viral antigens by immunohistochemistry, visualized by the 3,3′-diaminobenzidine tetrahydrochloride reaction (**c–f**). Arrows in a and b indicate the areas of spongiotic degeneration, which is a typical pathology in srr7 infection.[8] Arrowheads in a indicate cell infiltration beyond the Virchow-Robin space. White arrows in h and j indicate clustered and pyknotic cells, respectively. Black arrows in j indicate hemosiderin deposits. fBA and wBA indicate mutant and wild-type mice, respectively. dpi and hpi indicate days and hours post-inoculation with srr7, respectively. Scale bar: 100 (single line), or 20 μm (double line).
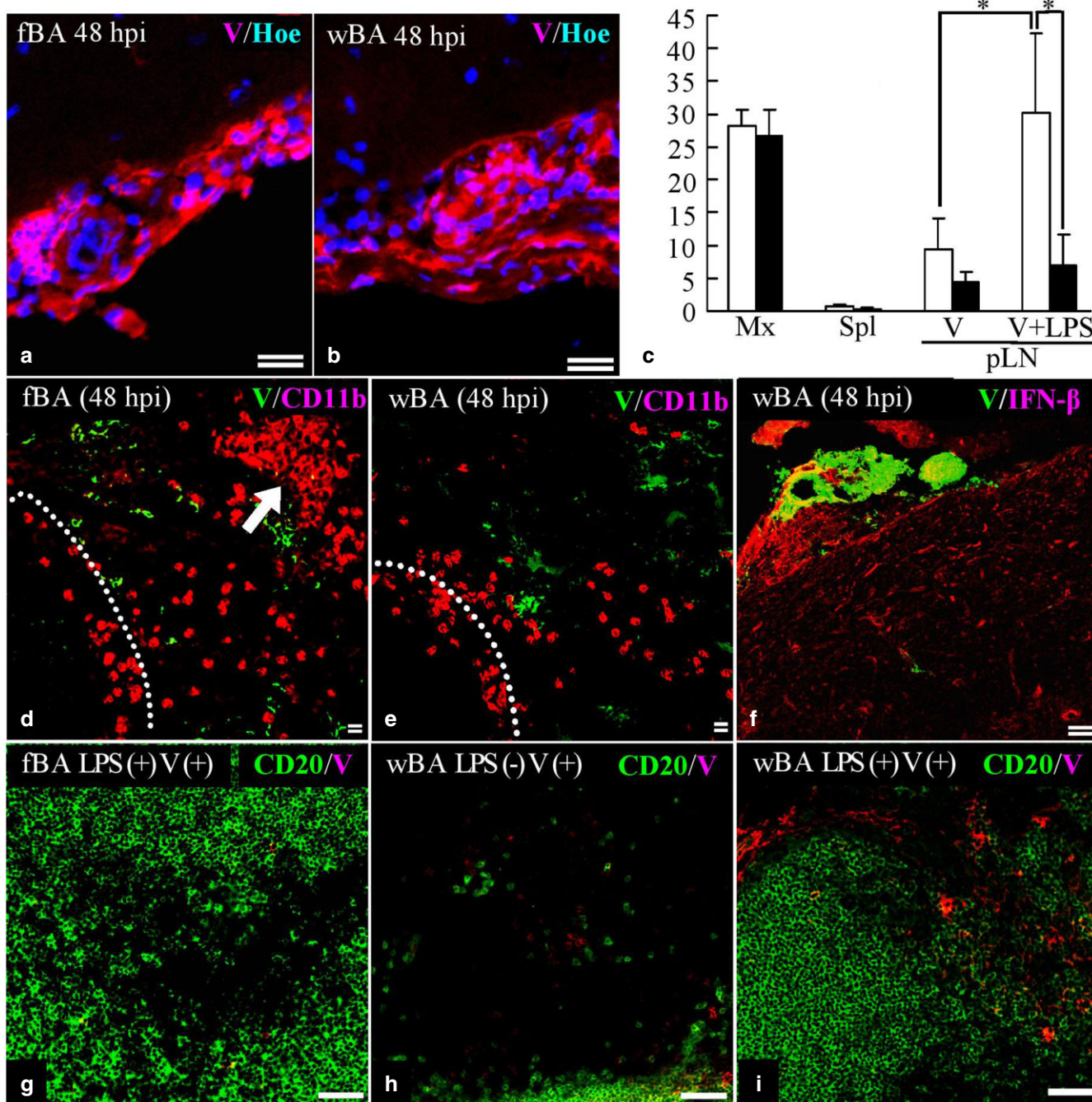
Figure 3 Frozen sections were stained for viral antigens (V), nuclei (Hoe), CD11b, CD20, and IFN-β by immunofluorescence in the meninges (**a,b**), pons (**f**), spleen (**d,e**), and popliteal lymph nodes (**g–i**) after inoculation with srr7 (V) and/or LPS. The areas surrounded by dotted lines in d and e include the follicles and marginal zones. The arrow in (**d**) indicates the nodular accumulation of CD11b-positive cells. Scale bar: 50 (single line), or 20 μm (double line). (**c**) The viral antigen-bearing cells and total cell numbers were quantified in frozen sections stained for viral antigens and nuclei by immunofluorescence, using a BZ-analyzer (Keyence). Ratios of viral antigen-bearing cells to total cell numbers in the sections of the meningeal region around the pons and cerebellum (Mx) and the spleen (Spl) are shown. The average number of viral antigen-positive cells in the section of popliteal lymph nodes (pLN) 48 h after treatment with srr7 (V) and/or LPS were also quantified. The standard deviation is shown by the vertical line. *P*-values (p) by Student's t-test is shown as *, which indicates $0.005 < P < 0.05$. fBA and wBA indicate mutant and wild-type mice, respectively. hpi indicates hours post-inoculation with srr7. ■, fBA; □, wBA.
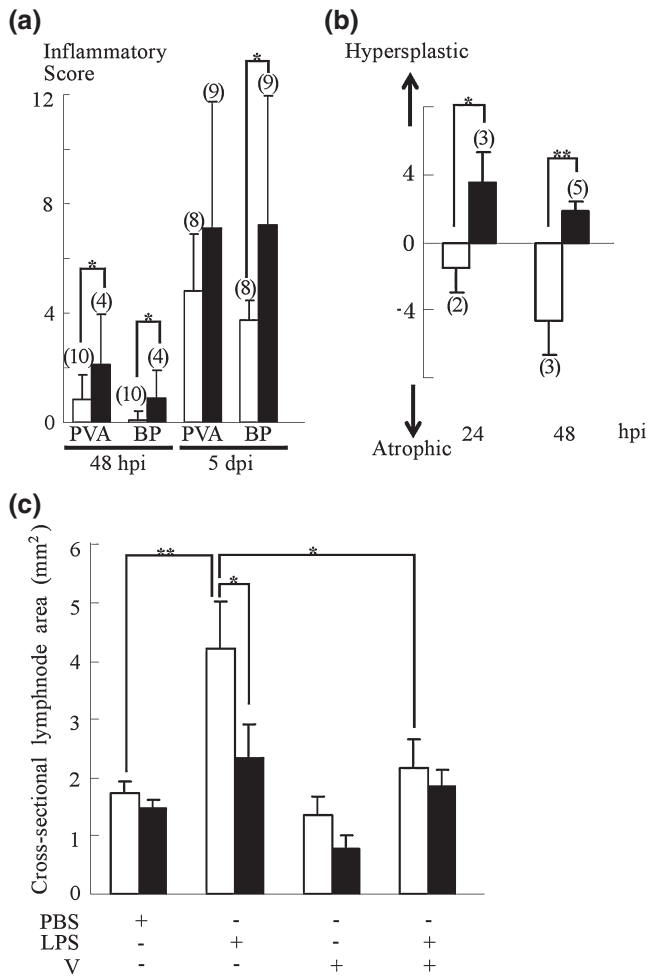
Figure 4 Pathological changes in the brain (**a**), spleen (**b**), and popliteal lymph nodes (**c**) of mutant (fBA, closed bars) and wild-type (wBA, open bars) mice were scored (**a,b**) or measured (**c**) as described in Methods. The numbers of animals are shown in parentheses (**a,b**), and the data are expressed as the average values obtained from the mice examined (**a–c**). (**a**) The intensities of inflammation were scored separately either in the perivascular area (PVA) within the Virchow-Robin space or in the brain parenchyma (BP) at 48 hpi and 5 dpi. The sums of scores obtained from five areas of the brain are shown. (**b**) The sums of hyperplastic and atrophic scores, scored as positive and negative points, respectively, are shown. The vertical axis corresponds to the normoplastic spleen. (**c**) Average lymph node areas were obtained from three mice per group at 48 hpi with LPS or PBS and/or srr7 (V). The standard deviation is shown by the vertical line. P-values (p) by Student's t-test are shown as * and **, which indicate $0.005 < P < 0.05$ and $P < 0.005$, respectively.

DISCUSSION

Extended inflammation in the brain and the rather hyperplastic state in the spleen of infected mutant mice, accompanied by lower viral titration compared to wild-type mice, indicated that mutant mice are more advantageously equipped for viral replication inhibition or viral clearance through inflammatory responses during the early phase of infection than wild-type mice. This indicates that Le[x] structures play an inhibitory role

in inflammation during the acute phase of infection. The finding that viral titers in mutant mice in the brain and liver after infection were lower than those in wild-type mice might be due to the lower infectivity of cells lacking Le[x] structures, because the major viral receptor, CEACAM1, carries Le[x] structures.[17] However, *in vivo* and *in vitro* examinations revealed that there was no difference in infectivity between wild-type and mutant mice. Therefore, the virological and pathological differences observed in the two strains would more likely result from different immune responses during the initial phase of infection.

Initial immune responses after infection are triggered by pathogen recognition through pattern recognition receptors (PRRs), which include Toll-like receptors (TLRs)[29] and various classes of glycan-binding receptor (lectins),[18,19] leading to the production of proinflammatory cytokines. A comparison of cytokine production between the two strains revealed that the amounts in the pons and spleen shifted after infection similarly in the two strains were less than 2-fold in almost every case. Therefore, similar survival rates in spite of different viral growth in the brains after infection in the two strains might be caused by the cytokine production being a bystander effect rather than directly due to the injury of infected cells. Bystander effects represented as an elevation of cytokine levels cause a poor prognosis after brain injuries observed in viral infection, such as influenza viral encephalopathy, which exhibits almost no inflammation nor viral growth in the brain,[20] and in other types of brain injury such as stroke.[30]

In the spleen, most of the cytokine levels examined in wild-type mice were reduced after infection more markedly than those in mutant mice. However, the differences in levels between wild-type and mutant mice were less than 2-fold in almost every case, which could also be a bystander effect in uninfected areas of the spleen, leading to elevated amounts of IFN-β in the whole spleen at 48 hpi both in wild-type and mutant mice, although it has been reported that MHV infection *in vitro* inhibits IFN-β-production.[26–28] There may be a more marked reduction of cytokine production in the spleen of wild-type mice compared to that of mutant mice in the local environment, especially in the interfollicular areas including the marginal zone, where viral antigens are detected during the early phase of infection,[6] and the influx and efflux of leukocytes are controlled through the fibroblastic reticular system.[31]

A difference in immediate inflammatory responses of the two strains was observed when mice were challenged by LPS, a ligand of TLR-4,[32,33] to induce lymphadenitis in the regional lymph nodes. In wild-type mice, the inflammatory response against LPS-challenge in the popliteal lymph nodes was tolerated after infection, which did not occur in mutant mice, as far as the size of the lymph nodes was concerned. LPS-tolerance, also known as endotoxin-tolerance,
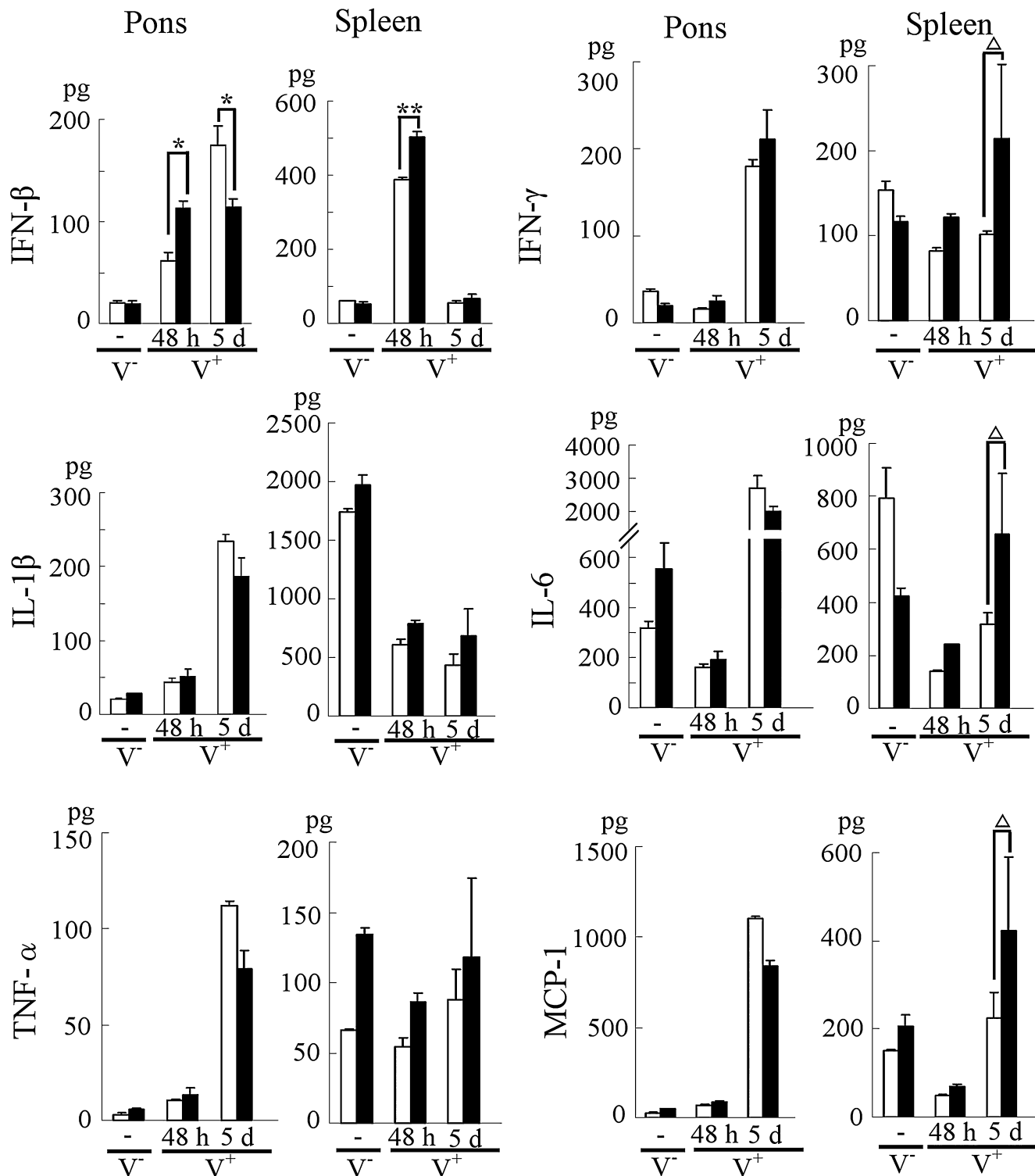
Figure 5 The amounts of cytokines in the pons and spleen obtained from uninfected (V⁻) and infected (V⁺) mice were measured. pg per 100 mg of tissue and per total organ, in the pons and spleen, respectively, are shown. fBA (closed bars) and wBA (open bars) indicate mutant and wild-type mice, respectively. d and h indicate days and hours post-inoculation with srr7, respectively. *P*-values (p) by Student's t-test are shown as **, *, and △, which indicate *P* < 0.005, 0.005 < *P* < 0.05, and 0.05 < *P* < 0.1, respectively.

is induced by LPS-challenge accompanied by other immunological treatments, infection, or injury,[34,35] and is caused by inhibitory cascades activated after the recognition of ligands by PRRs,[34,36] which play an important role in immunological homeostasis, suppressing excess immune responses activated through positive cascades triggered by the activation of PRRs.[36] The Le[x] structure might be involved in the negative cascades in the PRR pathway, causing more severe inflammation in the mutant mice after viral infection than in wild-type mice. The possibility that a lack of Le[x] causes increased inflammatory responses after up-regulation of the positive cascades in the PRR-pathway is unlikely, because mutant mice were refractory to *in vivo* challenge by LPS. Furthermore, most of the levels of cytokines examined after *in vitro* stimulation by LPS using leukocytes derived from naive mutant mice were lower or similar compared to those from wild-type mice. However, the production of IFNs was greater in the culture of leukocytes derived from mutant compared to wild-type mice, which excludes the possibility that mutant mice poorly recognize LPS.

Collectively, challenges by viral infection and/or LPS induced different inflammatory or immune responses between wild-type and mutant mice during the early phase after the challenges. The differences are not believed to be a result of different ligand-receptor affinities, but are more likely caused by differences in down-stream cascades, which are responsible for the down-regulation of excess immune responses triggered by the activation of PRRs.[36] Our experimental model would provide an opportunity to study the *in vivo* regulatory mechanism, which involves fucosylated glycans, causing the inhibition or enhancement of inflammation.

ACKNOWLEDGMENTS

REFERENCES

1   Bender SJ, Weiss SR. Pathogenesis of murine coronavirus in the central nervous system. *J Neuroimmune Pharmacol* 2010; **5**: 336–54.
2   Godfraind C, Langreth S, Cardellichio C *et al*. Tissue and cellular distribution of an adhesion molecule in the carcinoembryonic antigen family that serves as a receptor for mouse hepatitis virus. *Lab Invest* 1995; **73**: 615–27.
3   Nakagaki K, Nakagaki K, Taguchi F. Receptor-independent spread of a highly neurotropic murine coronavirus JHMV strain from initially infected microglial cells in mixed neural cultures. *J Virol* 2005; **79**: 6102–10.
4   Taguchi F, Siddell SG, Wege H, ter Meulen V. Characterization of a variant virus selected in rat brains after infection by coronavirus mouse hepatitis virus JHM. *J Virol* 1985; **54**: 429–35.
5   Saeki K, Ohtsuka N, Taguchi F. Identification of spike protein residues of murine coronavirus responsible for receptor-binding activity by use of soluble receptor-resistant mutants. *J Virol* 1997; **71**: 9024–31.
6   Takatsuki H, Taguchi F, Nomura R *et al*. Cytopathy of an infiltrating monocyte lineage during the early phase of infection with murinecoronavirus in the brain. *Neuropathology* 2010; **30**: 361–71.
7   Kashiwazaki H, Taguchi F, Ikehara Y, Watanabe R. Characterization of splenic cells during the early phase of infection with neuropathogenic mouse hepatitis virus. *Jpn J Infect Dis* 2011; **64**: 256–9.
8   Kashiwazaki H, Nomura R, Matsuyama S, Taguchi F, Watanabe R. Spongiform degeneration induced by neuropathogenic murine coronavirus infection. *Pathol Int* 2011; **61**: 184–91.
9   Kawase M, Shirato K, van der Hoek L, Taguchi F, Matsuyama S. Simultaneous treatment of human bronchial epithelial cells with serine and cysteine protease inhibitors prevents severe acute respiratory syndrome coronavirus entry. *J Virol* 2012; **86**: 6537–45.
10 de Groot RJ, Baker SC, Baric RS *et al*. Middle East respiratory syndrome coronavirus (MERS-CoV): Announcement of the Coronavirus Study Group. *J Virol* 2013; **87**: 7790–92.
11 Nomura R, Kashiwazaki H, Kakizaki M, Matsuyama S, Taguchi F, Watanabe R. Receptor-independent infection by mutant viruses newly isolated from the neuropathogenic mouse hepatitis virus srr7 detected through a combination of spinoculation and ultraviolet radiation. *Jpn J Infect Dis* 2011; **64**: 499–505.
12 Kakizaki M, Kashiwazaki H, Watanabe R. Mutant murine hepatitis virus-induced apoptosis in the hippocampus. *Jpn J Infect Dis* 2014; **67**: 9–16.
13 Kreisman LS, Cobb BA. Infection, inflammation and host carbohydrates: A Glyco-Evasion Hypothesis. *Glycobiology* 2012; **22**: 1019–30.
14 Watanabe R, Sawicki SG, Taguchi F. Heparan sulfate is a binding molecule but not a receptor for CEACAM1-independent infection of murine coronavirus. *Virology* 2007; **366**: 16–22.
15 de Haan CA, Li Z, te Lintelo E, Bosch BJ, Haijema BJ, Rottier PJ. Murine coronavirus with an extended host range uses heparan sulfate as an entry receptor. *J Virol* 2005; **79**: 14451–6.
16 Kudo T, Kaneko M, Iwasaki H *et al*. Normal embryonic and germ cell development in mice lacking alpha 1,3-fucosyltransferase IX (Fut9) which show disappearance of stage-specific embryonic antigen 1. *Mol Cell Biol* 2004; **24**: 4221–8.
17 Bogoevska V, Horst A, Klampe B, Lucka L, Wagener C, Nollau P. CEACAM1, an adhesion molecule of human granulocytes, is fucosylated by fucosyltransferase IX and interacts with DC-SIGN of dendritic cells via Lewis x residues. *Glycobiology* 2006; **16**: 197–209.
18 Rabinovich GA, van Kooyk Y, Cobb BA. Glycobiology of immune responses. *Ann N Y Acad Sci* 2012; **1253**: 1–15.
19 van Kooyk Y, Rabinovich GA. Protein-glycan interactions in the control of innate and adaptive immune responses. *Nat Immunol* 2008; **9**: 593–601.
20 Morishima T, Togashi T, Yokota S *et al*. Encephalitis and encephalopathy associated with an influenza epidemic in Japan. *Clin Infect Dis* 2002; **35**: 512–17.
21 Kudo T, Ikehara Y, Togayachi A *et al*. Expression cloning and characterization of a novel murine alpha1, 3-fucosyltransferase, mFuc-TIX, that synthesizes the Lewis x (CD15) epitope in brain and kidney. *J Biol Chem* 1998; **273**: 26729–38.
22 Kudo T, Fujii T, Ikegami S *et al*. Mice lacking alpha1,3-fucosyltransferase IX demonstrate disappearance of Lewis

x structure in brain and increased anxiety-like behaviors. *Glycobiology* 2007; **17**: 1–9.

23 Jiang XR, Song A, Bergelson S *et al*. Advances in the assessment and control of the effector functions of therapeutic antibodies. *Nat Rev Drug Discov* 2011; **10**: 101–11.

24 Okeley NM, Alley SC, Anderson ME *et al*. Development of orally active inhibitors of protein and cellular fucosylation. *Proc Natl Acad Sci U S A* 2013; **110**: 5404–9.

25 Matsuyama S, Watanabe R, Taguchi F. Neurovirulence in mice of soluble receptor-resistant (srr) mutants of mouse hepatitis virus: Intensive apoptosis caused by less virulent srr mutant. *Arch Virol* 2001; **146**: 1643–54.

26 Roth-Cross JK, Martinez-Sobrido L, Scott EP, Garcia-Sastre A, Weiss SR. Inhibition of the alpha/beta interferon response by mouse hepatitis virus at multiple levels. *J Virol* 2007; **81**: 7189–99.

27 Roth-Cross JK, Bender SJ, Weiss SR. Murine coronavirus mouse hepatitis virus is recognized by MDA5 and induces type I interferon in brain macrophages/microglia. *J Virol* 2008; **82**: 9829–38.

28 Rose KM, Elliott R, Martinez-Sobrido L, Garcia-Sastre A, Weiss SR. Murine coronavirus delays expression of a subset of interferon-stimulated genes. *J Virol* 2010; **84**: 5656–69.

29 Hauwel M, Furon E, Canova C, Griffiths M, Neal J, Gasque P. Innate (inherent) control of brain infection, brain inflammation and brain repair: The role of microglia, astrocytes, 'protective' glial stem cells and stromal ependymal cells. *Brain Res Brain Res Rev* 2005; **48**: 220–33.

30 Vartanian KB, Stevens SL, Marsh BJ, Williams-Karnesky R, Lessov NS, Stenzel-Poore MP. LPS preconditioning redirects TLR signaling following stroke: TRIF-IRF3 plays a seminal role in mediating tolerance to ischemic injury. *J Neuroinflammation* 2011; **8**: 140.

31 Bajenoff M, Egen JG, Koo LY *et al*. Stromal cell networks regulate lymphocyte entry, migration, and territoriality in lymph nodes. *Immunity* 2006; **25**: 989–1001.

32 Blasius AL, Beutler B. Intracellular toll-like receptors. *Immunity* 2010; **32**: 305–15.

33 Song DH, Lee JO. Sensing of microbial molecular patterns by Toll-like receptors. *Immunol Rev* 2012; **250**: 216–29.

34 Peng Q, O'Loughlin JL, Humphrey MB. DOK3 negatively regulates LPS responses and endotoxin tolerance. *PLoS One* 2012; **7**: e39967.

35 Sato S, Takeuchi O, Fujita T, Tomizawa H, Takeda K, Akira S. A variety of microbial components induce tolerance to lipopolysaccharide by differentially affecting MyD88-dependent and -independent pathways. *Int Immunol* 2002; **14**: 783–91.

36 Murray PJ, Smale ST. Restraint of inflammatory signaling by interdependent strata of negative regulatory pathways. *Nat Immunol* 2012; **13**: 916–24.

SUPPORTING INFORMATION

Additional Supporting Information may be found in the online version of this article at the publisher's web-site:

Methods S1 This file describes the detailed methods for evaluating the intensities of inflammation of the brain and hyperplastic or atrophic states of the spleen, and cytokine assay used in the study.

Figure S1 The amounts of cytokines in the culture supernatant derived from uninfected wild-type (wBA) or mutant (fBA) mice, after stimulation with LPS (/LPS) or medium (/Medium), were measured. *P*-values (p) by Student's t-test are shown as ** and * which indicate $P < 0.005$ and $0.005 < P < 0.05$, respectively.